Existence of triply charged actinide-hydride molecules

Johannes Lachner,* Marcus Christl, Christof Vockenhuber, and Hans-Arno Synal
Laboratory of Ion Beam Physics, ETH Zurich, Switzerland

Xiaoyan Cao-Dolg and Michael Dolg
Institute for Theoretical Chemistry, University of Cologne, Germany
(Received 21 December 2011; published 28 February 2012)

Molecules consisting of actinide elements (Th, U) and hydrogen were detected as diatomic trications using low-energy accelerator mass spectrometry (AMS). In many AMS setups the molecules are destroyed by sending a negative ion beam through a foil or a gas medium (the so-called stripper) and by selecting ions in charge state 3+ or higher afterwards. During measurements of samples containing the abundant isotopes ^{232}Th, ^{235}U, and ^{238}U, a stripper thickness dependent counting rate on the next higher mass, i.e., 233, 236, and 239, was observed when selecting the 3+ charge state. The dependence of the signal intensity on the thickness of the stripper gas indicates a partial survival of triply charged molecules of mass 233, 236, and 239, respectively. In a dedicated experiment, the existence of the molecule $^{232}ThH^{3+}$ could be verified by directly detecting the breakup fragment $^{232}Th^{3+}$. Quantum chemical *ab initio* calculations at the scalar-relativistic complete active space self-consistent field (CASSCF) and multireference configuration interaction (MRCI) level confirm the existence of both ThH^{3+} and UH^{3+} by revealing local minima on the potential curves.

DOI: 10.1103/PhysRevA.85.022717 PACS number(s): 34.70.+e, 29.20.Ej, 07.75.+h

I. INTRODUCTION

Mass spectrometric measurements showed the existence of molecular trications for the first time in 1964. The first detected candidates were found to be built up from three or four constituents (CS_2^{3+}, COS^{3+}, and $C_2N_2^{3+}$) [1]. The existence of these relatively light triply charged molecules was explained by the number of nonbonding or delocalized electrons. Along with two other triply charged triatomic molecules (CS_2^{3+}, CSe_2^{3+}) the first diatomic trication (S_2^{3+}) was found 20 years later [2]. Further, using ultrashort-pulse strong-field multiphoton ionization it was demonstrated that halogen elements build metastable diatomic trications like I_2^{3+}, Br_2^{3+}, and Cl_2^{3+} [3]. By applying electron ionization of UF_6, the triply charged molecular ion UF^{3+} was produced [4], which was up to now the only reported diatomic trication containing an actinide element.

The lightest diatomic trication [$(^{11}B^{10}B)^{3+}$] was observed at a Tandem accelerator [5]. However, until recently an influence of triply charged molecules on measurements using accelerator mass spectrometry (AMS) has not been considered [6]. Instead, the choice of the charge state 3+ was thought to guarantee a Coulomb dissociation [7,8] and thereby the complete removal of all molecular background in any relevant case. In particular for low-energy AMS of actinides the charge state 3+ is commonly used because of its high yield after interaction of the negative ion beam with the stripper medium [9,10].

In this paper we present the detection of AnH^{3+} (An = Th,U) molecules by means of AMS. Further, we discuss results of quantum chemical *ab initio* calculations for the AnH^{3+} potential curves and the geometry of the $ThOH^-$ precursor molecule.

*lachner@phys.ethz.ch

II. EXPERIMENTAL METHOD

The setup of the ETH-Tandy AMS system for actinide measurements is described in detail elsewhere [11]. Here only the main setup and some specific methods relevant for the detection of the molecular breakup fragment are described.

A. Experimental setup

In a Cs sputter ion source negative molecular and atomic ions are extracted from targets of ThO_2 or UO_2 mixed with Fe_2O_3 and/or Nb powder. AnO^- molecules (along with possible traces of $AnOH^-$ or other molecules of the same mass) are filtered according to their mass by a magnet on the low-energy (LE) side and then are injected into the tandem accelerator running at a terminal voltage of about 300 kV. At the terminal of the accelerator the ion beam passes through a gas filled canal, the so-called stripper. The measurements presented here were performed using Ar as a stripper gas. Later measurements with He showed similar results. In the stripper, electrons are removed from the beam and molecules are destroyed by multiple collisions with the stripper gas, so that mainly positively charged ions (1+, 2+, 3+, . . .) leave the accelerator. The high-energy (HE) side consists of three m/q sensitive filters [first HE magnet (HE1), electrostatic analyzer (ESA), and second HE magnet (HE2)]. In the routine setup for actinides the 3+ charge state is selected with all three devices. On the HE side the ions are filtered first according to their p/q ratio by the HE1 magnet and then according to their E/q ratio in the ESA. The HE2 magnet provides a second p/q selection. The ions are detected in a gas ionization chamber.

After the HE1 magnet a SiN foil may be inserted at the position of the focal plane, which allows a second stripping process of the ion beam, called poststripping. The following mass spectrometer (ESA and HE2 magnet) is constructed such that the energy and angular straggling of the beam is largely compensated by its achromatic and angular focusing

TABLE I. U samples used for the stripper scans.

Material	Nominal $^{236}U/^{238}U$ ratio	Ref.
ZUTRI	$(4.05 \pm 0.10) \times 10^{-9}$	in house
Vienna-KkU	$(6.98 \pm 0.32) \times 10^{-11}$	[13]
LOT2061	$(6.05 \pm 0.44) \times 10^{-12}$	[13]

characteristics [12]. The poststripping option is not used during routine measurements of actinides with the Tandy.

For this study, the standard setup for actinide measurements was modified in a way that allows one to destroy any surviving molecules after the stripper and to analyze their breakup products. Therefore the SiN poststripping foil was replaced by a very thin (2 μg/cm^2) diamondlike carbon (DLC) foil. The molecular breakup products were analyzed in the following combination of ESA and HE2 magnet. The thin DLC foil was chosen for the poststripping process in order to minimize angular and energy straggling in the foil.

Because of the large masses of the actinides, the relative mass difference between neighboring nuclides is small. Therefore abundant neighboring nuclides may generate background from energy loss, scattering, or charge changing events in the mass spectrometer. A sensitive determination of rare radionuclides then is only possible in a setup with high mass suppression.

Surviving isobaric molecules (e.g., ^{235}UH or ^{238}UH) with the mass of the rare isotopes (e.g., ^{236}U or ^{239}Pu) may account for an additional counting rate in the detector. In our experiment we focused on the detection of ThH^{3+}. Poststripping of the beam was used to destroy the ThH^{3+} molecules, which had survived the stripping process in the accelerator, and to search for the fragment Th^{3+}. The two molecule fragments are extremely asymmetric in their masses. The relative mass difference between the molecule (ThH^{3+}) and the heavy breakup fragment (Th^{3+}) thus is very small, which makes their separation challenging.

B. Samples

The experiments to detect ThH^{3+} (Sec. III) were performed on targets with ThO_2 produced from a $TH(NO_3)_4$ standard solution (Alfa Aesar Lot No. 13911065). In the course of the measurements at 236 and 239 atomic mass units (amu) three different U samples were used that have a known $^{236}U/^{238}U$ ratio (Table I).

III. RESULTS

The existence of AnH^{3+} molecules is deduced from three independent experimental findings. First, stripper gas pressure-dependent counting rates were detected one mass unit above ^{232}Th, ^{235}U, and ^{238}U. These counting rates (^{233}X, ^{236}X, ^{239}X) represent a background for regular AMS measurements at masses 236 [Fig. 1(a)], 239 [Fig. 1(b)], and 233 (Fig. 2), respectively, and can be attributed to the survival of actinide-hydride molecules. The survival rate of molecules passing through the stripper is a function of the stripper gas pressure and hence the stripper thickness. This was previously studied for single positively charged ions [14] and double positively charged ions [15]. In all cases of partial survival of molecules in the beam an exponential decrease of the background counting rates with increasing target thickness was observed. This dependence of the signal intensity on the thickness of the stripper gas indicates the molecular character of the background counting rates in our actinide measurements.

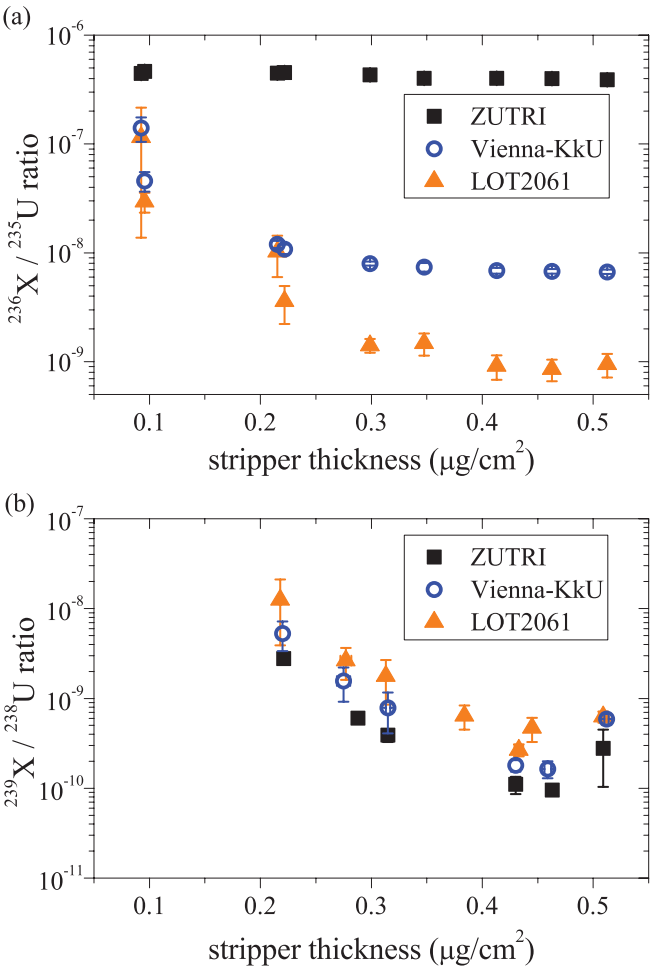

FIG. 1. (Color online) (a) The $^{236}X/^{235}U$ ratio (counting rate/counting rate) as a function of Ar stripper gas thickness for three different samples. The nominal $^{236}U/^{238}U$ ratios of the samples are given in Table I. The ^{235}U rate is calculated from the ^{238}U current measured after the HE1 magnet, assuming the natural ratio $\frac{^{235}U}{^{238}U} = 0.0726$. (b) The exponential decrease of the counting rate at 239 amu relative to the ^{238}U current is shown as a function of Ar stripper gas thickness for the samples described in Table I. The ratio at a stripper thickness of 0.6 μg/cm^2 is higher than the values between 0.4 and 0.5 μg/cm^2. Most likely, these variations in the background arise from time-dependent actinide-hydroxide molecule formation in the target.

Second, any contribution from scattered neighboring abundant isotopes to the increased counting rate at the mass of the rare isotopes could be excluded by measurements with a time-of-flight (TOF) detector, which was temporarily installed at the AMS system [11].

Third, it could further be ruled out that the increased counting rates from targets containing materials with a low $^{236}U/^{238}U$ ratio resulted from contamination with ^{236}U or from

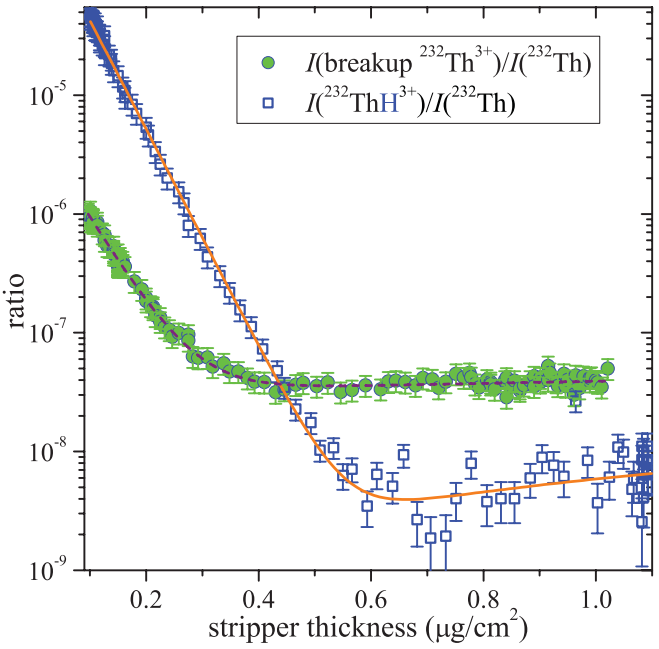

FIG. 2. (Color online) The counting rate at mass 233 relative to the $^{232}Th^{3+}$ current after the HE1 magnet decreases exponentially as a function of the Ar stripper gas thickness (blue open squares) until the background level of the measurement is reached. In the setup with the poststripping foil, $^{232}Th^{3+}$ from the breakup is detected and again normalized to the $^{232}Th^{3+}$ HE current (green circles). The exponential decrease of $^{232}Th^{3+}$ from the breakup is visible only up to a stripper thickness of 0.25 $\mu g/cm^2$, but the slope is comparable to the one of the molecular background. In the foil experiment the background level is shifted upward because of the worse separation on the HE side of the spectrometer. For both cases, with and without foil, the raw measured isotopic ratios are shown without any correction for possible beam losses between the HE cup and the detector. The data are fitted with a superposition of an exponential and a linear function.

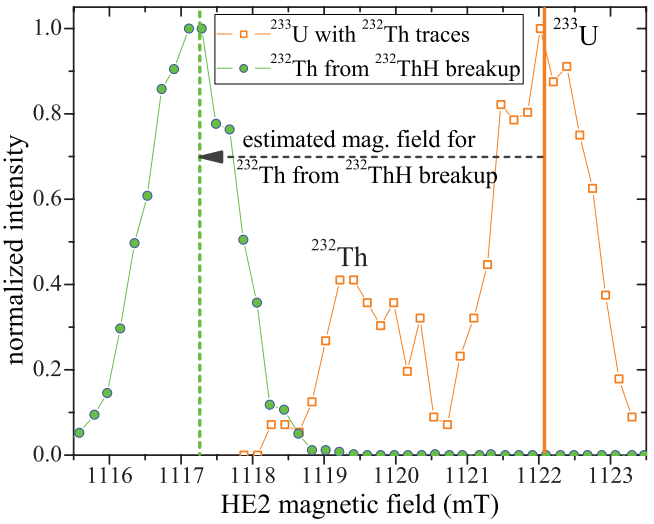

FIG. 3. (Color online) To demonstrate that breakup ^{232}Th can be separated from the original mass 233 molecule, scans of the HE2 magnet on targets containing ^{233}U (at ESA = 22.33 keV, orange open squares, the straight orange line marks the optimum value) and ^{232}Th (at ESA = 22.23 keV, green circles) are shown at a stripper thickness of 0.16 $\mu g/cm^2$. The ^{232}Th traces in the ^{233}U sample are separated in the HE2 magnet, as from the ESA one energy is defined $E_{232} = E_{233}$, which results in a lower momentum for the ^{232}Th compared to the ^{233}U. The green dashed line marks the expected magnetic field for $^{232}Th^{3+}$ from $^{232}ThH^{3+}$ breakup at the according ESA settings. Counting rates were normalized to allow a better comparison between the two settings.

isobars like ^{236}Np and ^{236}Pu, because the observed counting rate at 236 amu still depended on the stripper thickness.

Tests with ^{232}Th showed that the survival rate of ThH^{3+} molecules (blue open squares in Fig. 2) is significantly larger compared to UH^{3+}. To identify ThH^{3+} unambiguously, a beam at 233 amu was poststripped in a thin DLC foil after the accelerator to break up the suspected molecule into its constituents H and Th. In the following it is described how the fragment Th^{3+} was identified and how the existence of $^{232}ThH^{3+}$ was confirmed.

The energy loss in the poststripping foil reduced the beam energy by approximately 60 keV and new settings for the ESA and the HE2 magnet had to be determined. A beam of ^{233}U (Fig. 3) was used to determine the energy loss in the foil and to find the new settings for ThH. This implies that U has the same energy loss in the foil as Th. Calculations using the program SRIM [16] confirmed that the difference in energy loss of 1.26-MeV U and Th ions in C is so small (0.2% of the total beam energy) that it cannot be resolved by the following spectrometer. Using the experimentally determined ^{233}U settings for the ESA and the HE2 magnet as a reference (orange open squares in Fig. 3 with the straight orange line marking the value of the HE2 magnet for 233 amu) the new settings are calculated from the kinematics of the expected ThH^{3+} breakup into a Th^{3+} and hydrogen (energy: $E_{233} = E_{232,\text{breakup}} + E_1$ and momentum: $p_{233} = p_{232,\text{breakup}} + p_1$). The $^{232}Th^{3+}$ originating from the breakup must have a lower energy ($E_{232,\text{breakup}} = \frac{232}{233} \times E_{233}$) and a lower momentum ($p_{232,\text{breakup}} = \frac{232}{233} \times p_{233}$). Analyzing a beam at 233 amu extracted from a ThO_2 sample with the DLC poststripping foil and applying the settings calculated for the ThH breakup (green dotted vertical line marking the calculated value of the HE2 magnet in Fig. 3) to the ESA and the HE2 magnet, a beam of nuclides at mass 232 was found.

The counting rate at these settings (green circles in Fig. 2) showed the same stripper pressure-dependent behavior as it did under the influence of the molecular background (blue squares in Fig. 2). From the similar exponential decrease of the counting rates in the region of lower stripper thicknesses ($<0.3\ \mu g/cm^{-2}$) we conclude that the counting rate at 232 amu originates from the breakup of a molecule at mass 233. The data are fitted with the function $f(d) = \alpha \cdot e^{-\sigma \cdot d} + \beta \cdot d + \gamma$, d being the stripper thickness. This fit describes the exponential decrease of molecular background with increasing stripper pressure and a linear contribution from other sources of background [6]. The decay constant σ corresponds to the cross section for the destruction of the molecules in the Ar stripper gas. From the fits to the ThH^{3+} counting rate and to the breakup Th^{3+} counting rate in Fig. 2 this cross section can be deduced to $1.4 \times 10^{-15}\ cm^2$ and $1.2 \times 10^{-15}\ cm^2$, respectively.

Because of the energy and angular straggling in the foil, the $^{232}Th^{3+}$ beam from the breakup has a larger divergence.

The transmission of the beam from the foil through ESA, the following slits, and the HE2 magnet into the detector therefore is much lower than it is for the beam not interacting with the foil. This results in a lower counting rate in the region where the exponential decrease dominates (Fig. 2, 0–0.3 μg/cm^2). However, with the foil inserted into the beam, the background level for higher stripper pressures is shifted upward by a factor of 10 (Fig. 2, 0.3–1.0 μg/cm^2). The increased counting rate in the foil setup at higher stripper pressures is most probably caused by the scattering processes in the foil and the enhanced tailing of the more intense $^{232}Th^{3+}$ beam: The HE1 magnet does not completely filter $^{232}Th^{3+}$ out of the beam at mass 233. In this setting, scattered $^{232}Th^{3+}$ ions that are not further suppressed by the ESA are also not separated in the HE2 magnet so that they will appear also at the HE2 magnetic field marked by the dashed green vertical line in Fig. 3.

An attempt to detect the hydrogen from the breakup using a Channeltron detector positioned after the ESA was not successful. The proton beam would have been expected at an energy of only 5.4 keV. However, no distinct peak was found at this energy when scanning the ESA, possibly because of the large angular divergence of the protons caused by the Coulomb dissociation in the foil. In addition, at these low beam energies a significant amount of the hydrogen might be neutral after the breakup and the interaction with the foil, which would also explain the missing occurrence of a proton beam.

IV. DISCUSSION

A. Implications of the experimental results

Molecules of actinides and hydrogen were observed in charge state 3+. In our experiment, the oxygen of the $AnOH^-$ molecules is removed during the stripping to charge state 3+, whereas surprisingly the actinide-hydrogen bond is not destroyed at the same time. The calculations presented in the next section show that the hydrogen can be directly bound to the actinides and is not preferentially present in an OH molecule where no bonding exists between the hydrogen and the actinide.

The relatively constant background levels observed at higher stripper thicknesses originate most likely from scattered abundant isotopes that were injected into the accelerator as $AnOH^-$ molecules and that were extracted as a An^{3+} ion. Assuming a similar hydride formation rate, the ratios of all background levels relative to the abundant isotopes are expected to be the same. However, different absolute values of the background levels are observed for $^{233}X/^{232}Th$, $^{236}X/^{235}U$, and $^{239}X/^{238}U$. In all measured U samples there are traces of real ^{236}U. Consequently, if one wants to study the 236 background for the lowest sample LOT2061, the nominal $^{236}U/^{235}U$ ratio (8.3×10^{-10}) has to be substracted from the measured one (13.0×10^{-10}) to compare the background ratios $^{236}X/^{235}U$ and $^{239}X/^{238}U$ to show their consistency. Still, compared to the background levels one mass unit above the abundant U isotopes, the background for mass 233 relative to the ^{232}Th intensity is higher. This can be explained if the $AnOH^-$ formation rate in the ion source is higher for Th than for U. Such a difference in the formation rates would also be in agreement with the larger ThH^{3+} survival rate observed at lower stripper thicknesses.

The results of the experiments showed that the formation rates of the initial negative $AnOH^-$ molecular ions and the survival rates of the triply charged actinide-hydride molecular ions (AnH^{3+}) depend on the actinide element.

B. Quantum chemical calculations

Correlated quantum chemical *ab initio* calculations were performed for ThH^{3+} and UH^{3+} at the complete active space self-consistent field (CASSCF) level, followed by multireference configuration interaction (MRCI), using the MOLPRO program system [17–19]. Relativistic effects were included by means of scalar-relativistic energy-consistent small-core pseudopotentials for Th [20] and U [21]. Atomic natural orbital (ANO) valence basis sets using up to g functions were applied for Th and U [21,22], whereas the augmented polarized correlation-consistent valence quadruple-ζ (aug-cc-pVQZ) set of Dunning [23] containing up to f functions was applied for H. The active orbital space comprised the An $5f$, $6d$, $7s$, and H $1s$ orbitals. At the MRCI level excitations were allowed from these orbitals as well as from An $6s$ and $6p$, whereas the An $5s$, $5p$, and $5d$ shells were kept frozen. The CASSCF calculations considered the low-lying singlet and triplet states of ThH^{3+} as well as the low-lying triplet and quintet states of UH^{3+}. Only the lowest states were thereafter investigated at the MRCI level as representatives of a large number of nearly degenerate electronic states resulting at the CASSCF level. Spin-orbit effects were not included since they are not expected to lead to qualitative or major quantitative changes.

The calculated potential curves of ThH^{3+} and UH^{3+} are displayed in Figs. 4 and 5, respectively. Both molecules dissociate in An^{2+} and H^+, since the third ionization potentials of the actinide elements (Th: 18.33 ± 0.05 eV, U: 19.80 ± 0.31 eV) [24] are larger than the one of hydrogen (13.61 eV). The crossing of the repulsive $An^{2+} + H^+$ asymptote with the potential curves corresponding to a $An^{3+} + H$ charge distribution occurs at about 6 Å. In case of ThH^{3+} the $^1\Sigma$ curve corresponding to a Mulliken charge distribution $Th^{2.93+}$ $5f^{0.21}$ $6d^{0.68}$ $7s^{0.16}$ $7p^{0.03}$ $H^{0.07+}$ $1s^{0.88}$ $2p^{0.04}$ exhibits a clear minimum at 1.888 Å, characterized by a vibrational constant of 1830 cm^{-1}. The bond between Th and H may be regarded as a σ bond formed by two electrons with main contributions of Th $6d$ and H $1s$. The local minimum of the ThH^{3+} potential curve is about 2.25 eV above the dissociation limit. At intermediate distances between 3.5 and 6 Å the charge distribution corresponds roughly to Th^{3+} $5f^1 + H$ $1s^1$. The energy barrier toward the dissociative $Th^{2+} + H^+$ potential curves amounts to about 2.26 eV. The lowest ThH^{3+} triplet potential curve exhibits only a relatively weak local minimum with a $Th^{2.81+}$ $5f^{0.97}$ $6d^{0.13}$ $7s^{0.04}$ $7p^{0.04}$ $H^{0.19+}$ $1s^{0.79}$ $2p^{0.02}$ charge distribution. The singlet and triplet asymptotes for large internuclear distances are very similar in energy, since at the present level of theory Th^{2+} $5f^1$ $6d^1$ ^1G is only 0.04 eV above the $6d^2$ ^3F ground state.

In comparison to ThH^{3+} the metastable character of UH^{3+} is less pronounced. The $^5\Phi$ potential curve exhibits a minimum at 2.649 Å with a vibrational constant of 708 cm^{-1}. The Mulliken charge distribution near the minimum

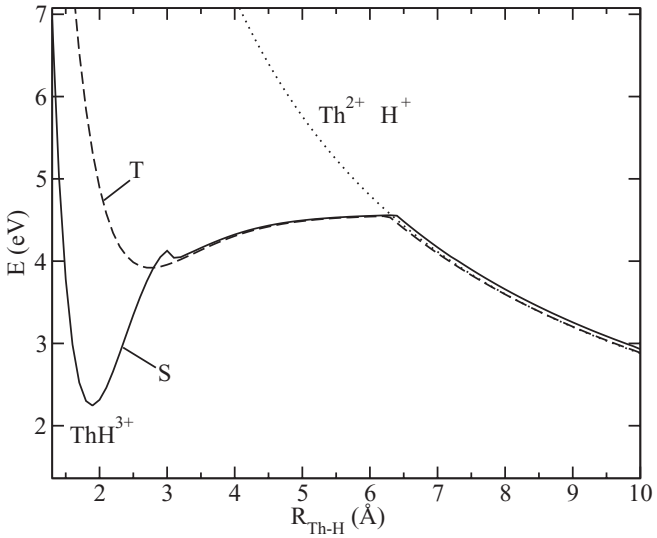

FIG. 4. ThH^{3+} potential energy relative to the distance R of the two molecular partners. S and T denote the lowest singlet and triplet curves, respectively.

is $U^{2.78+}\ 5f^{3.02}\,6d^{0.10}\,7s^{0.06}\,7p^{0.05}\ H^{0.22+}\ 1s^{0.76}\,2p^{0.02}$. The local minimum is located about 4.13 eV above the energy of the separated U^{2+} and H^{+} ions, and the barrier to dissociation is about 0.60 eV, both indicating a higher instability than for ThH^{3+}. One reason is the about 1.5 eV higher third ionization potential of U compared to the one of Th, which shifts the bound An^{3+}H curves up relative to the purely repulsive An^{2+} + H^{+} curves. In addition, the valence electrons on U are localized in the $5f$ shell, which is more corelike than for Th, and do not contribute much to covalent bonding. The main bonding interaction between H and U arises from a σ bond formed by one electron with the main contribution from H $1s$, and a smaller one from U $6d$. Nearly degenerate, i.e., only about 0.10 eV higher in energy, is the minimum of the $^3\Phi$ potential curve at 2.700 Å with a vibrational constant of 654 cm^{-1} and an

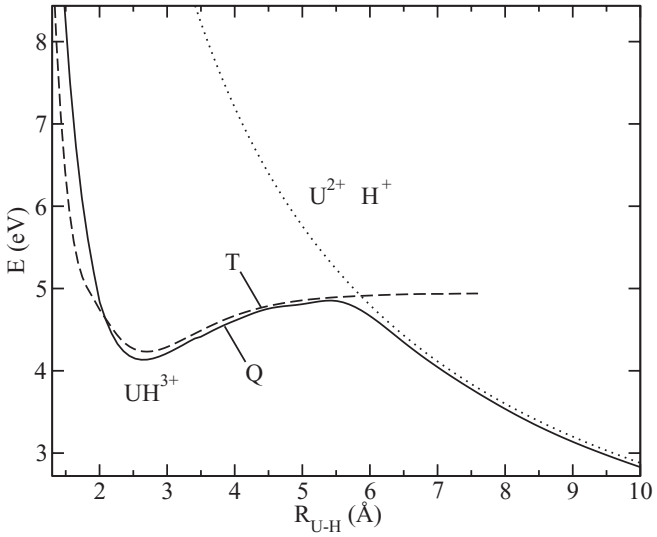

FIG. 5. UH^{3+} potential energy relative to the distance R of the two molecular partners. T and Q denote the lowest triplet and quintet curves, respectively.

almost identical charge distribution. At intermediate distances between 4.5 and 5.5 Å the charge distribution corresponds roughly to $U^{3+}\ 5f^3\ +\ H\ 1s^1$. The lowest asymptotes for large internuclear distances arise only from quintet states. At the present level of theory $U^{2+}\ 5f^3\,6d^1\,{}^5L$ is the ground state and $5f^4\,{}^5I$ and $5f^3\,7s^1\,{}^5I$ states are located at 0.23 and 0.37 eV, respectively, whereas the lowest triplet state arising from $5f^3\,6d^1$ is located at 0.43 eV. It should be noted that a quantitatively accurate description of the atomic energy levels requires more extended correlation treatments using still larger one-particle basis sets as well as the inclusion of spin-orbit interaction [21,25].

The question of the structure of the precursor molecules was further investigated for Th at the CASSCF and CASSCF-MRCI level. Dunning's aug-cc-pVQZ basis set containing up to g functions was used for O [23], whereas the Th and H basis sets were as stated above. In a first step we investigated a linear approach of H$^-$ to ThO at the CASSCF level. Linear HThO$^-$ in its lowest singlet state was found to be by 0.33 and 1.69 eV lower in energy than the lowest triplet and singlet states of linear ThOH$^-$, respectively, thus supporting a stronger interaction of H with Th than with O. The triplet and quintet states of linear HThO$^-$ are about 0.96 and 3.37 eV, respectively, higher in energy than the singlet ground state. As a second step full geometry optimizations were performed at the CASSCF/MRCI level. Here HThO$^-$ turns out to be strongly bent with a $^1A'$ ground state [R(Th-H) = 2.170 Å, R(Th-O) = 1.869 Å, ∠(H-Th-O) = 106.6°]. The lowest excited states are $^3A''$ [R(Th-H) = 2.189 Å, R(Th-O) = 1.874 Å, ∠(H-Th-O) = 107.2°] and $^3A'$ [R(Th-H) = 2.222 Å, R(Th-O) = 1.880 Å, ∠(H-Th-O) = 111.6°] with term energies of 0.88 and 0.97 eV, respectively. The lowest electronic states of structures corresponding to ThOH$^-$ turned out to be more than 2 eV above the HThO$^-$ $^1A'$ ground state. Thus quantum chemical results support a direct bonding of H to the actinide in the precursor molecules.

V. CONCLUSIONS

The existence of UH^{3+} and ThH^{3+} molecules could be demonstrated using the low-energy AMS system Tandy. Counting rates at masses 233, 236, and 239, which were exponentially decreasing with increasing stripper thickness, indicated the survival of ^{232}ThH^{3+}, ^{235}UH^{3+}, and ^{238}UH^{3+} molecules after collisions with Ar gas in the stripper canal. Using a TOF detector, it could be resolved that indeed real mass 236 arrives at the detector and that the increased counting rates are not due to scattered abundant isotopes. An experiment was conducted to break up the ThH^{3+} molecule and to detect the heavier molecular breakup product ^{232}Th^{3+}. The extremely asymmetric mass distribution in this molecule makes such an experiment highly challenging, as the energy of the heavy breakup product is only marginally (8.7×10^{-3}) shifted relative to the total beam energy and the energy of the hydrogen was too low to allow a detection. Only the high abundance sensitivity of the Tandy AMS setup in combination with the use of a thin poststripping foil facilitates such a separation of the breakup product.

Taking into account the time the ions need from the charge transfer in the stripper to the detector, a minimum lifetime of

10 μs for the 3+ actinide-hydride molecules can be deduced. This implies that these molecules are at least metastable.

Relativistic electronic structure calculations support the existence of ThH^{3+} and UH^{3+} as metastable molecular ions. For ThH^{3+} the quantum chemical calculations show that Th and H are bound by a σ bond formed by two electrons. The local minimum of ThH^{3+} $^1\Sigma$ potential curve is separated from the dissociative $Th^{2+} + H^{1+}$ state by an energy barrier of 2.26 eV. Because the third ionization potential of U is higher than the one of Th and because the covalent σ bond between U and H is only realized by one electron, the theoretical calculations reveal that UH^{3+} is less metastable, which is also reflected by the lower counting rates for surviving UH^{3+} in the AMS measurement. The minima of the potential curves $^5\Phi$ and $^3\Phi$ are nearly degenerate, the minimum of the lower quintet state $^5\Phi$ has a barrier to dissociation into $U^{2+} + H^+$ of only 0.60 eV. In addition, it could be shown that the electronic ground state of $HThO^-$ is more than 2 eV lower than the lowest $ThOH^-$ states. This explains why an AnH^{3+} ion can survive after the O is removed from a precursor molecule of An, O, and H.

Further on, the findings also have implications for the practical use of the AMS technique, as measurements free of any molecular background are not guaranteed any more for actinides using the charge state 3+. Future developments of AMS in the 3+ charge state will have to consider the possible additional background at lower stripper densities arising from the survival of molecules. To investigate such background counting rates, experiments on other, lighter radionuclides measured in the charge state 3+ will also be conducted.

This study demonstrates that a positive evidence for the existence of 3+ molecules is qualitatively possible with such a setup, enabling also highly sensitive searches for other molecular trications.

[1] A. Newton, J. Chem. Phys. **40**, 607 (1964).

[2] L. Morvay and I. Cornides, Int. J. Mass Spectrom. **62**, 263 (1984).

[3] H. Sakai, H. Stapelfeldt, E. Constant, M. Y. Ivanov, D. R. Matusek, J. S. Wright, and P. B. Corkum, Phys. Rev. Lett. **81**, 2217 (1998).

[4] D. Schröder, M. Diefenbach, T. Klapötke, and H. Schwarz, Angew. Chem. Int. Ed. **38**, 137 (1999).

[5] D. Weathers, F. McDaniel, S. Matteson, J. Duggan, J. Anthony, and M. Douglas, Nucl. Instrum. Methods Phys. Res., Sect. B **56-57**, 889 (1991).

[6] J. Lachner, M. Christl, C. Vockenhuber, and H.-A. Synal, Nucl. Instrum. Methods Phys. Res., Sect. B, (2012), doi:10.1016/j.nimb.2012.02.010.

[7] K. Purser, A. Litherland, and J. Rucklidge, Surf. Interface Anal. **1**, 12 (1979).

[8] W. Kutschera, Int. J. Mass Spectrom. **242**, 145 (2005).

[9] L. Wacker, E. Chamizo, L. Fifield, M. Stocker, M. Suter, and H. Synal, Nucl. Instrum. Methods Phys. Res., Sect. B **240**, 452 (2005).

[10] E. Chamizo, S. M. Enamorado, M. García-León, M. Suter, and L. Wacker, Nucl. Instrum. Methods Phys. Res., Sect. B **266**, 4948 (2008).

[11] C. Vockenhuber, M. Christl, C. Hoffmann, J. Lachner, A. M. Müller, and H.-A. Synal, Nucl. Instrum. Methods Phys. Res., Sect. B **269**, 3199 (2011).

[12] A. Müller, M. Christl, J. Lachner, M. Suter, and H.-A. Synal, Nucl. Instrum. Methods Phys. Res., Sect. B **268**, 2801 (2010).

[13] P. Steier, M. Bichler, L. K. Fifield, R. Golser, W. Kutschera, A. Priller, F. Quinto, S. Richter, M. Srncik, P. Terrasi, L. Wacker, A. Wallner, G. Wallner, K. M. Wilcken, and E. M. Wild, Nucl. Instrum. Methods Phys. Res., Sect. B **266**, 2246 (2008).

[14] H.-A. Synal, M. Stocker, and M. Suter, Nucl. Instrum. Methods Phys. Res., Sect. B **259**, 7 (2007).

[15] H. Lee, A. Galindo-Uribarri, K. Chang, L. Kilius, and A. Litherland, Nucl. Instrum. Methods Phys. Res., Sect. B **5**, 208 (1984).

[16] J. Ziegler, J. Biersack, and U. Littmark, *The Stopping and Range of Ions in Solids* (Pergamon, New York, 1985).

[17] MOLPRO (version 2006.1) is a package of ab initio programs designed by H.-J. Werner and P.J. Knowles, [http://www.molpro.net].

[18] P. J. Knowles and H.-J. Werner, Chem. Phys. Lett. **115**, 5053 (1985).

[19] H.-J. Werner and P. J. Knowles, J. Chem. Phys. **89**, 5803 (1988).

[20] W. Küchle, M. Dolg, H. Stoll, and H. Preuß, J. Chem. Phys. **100**, 7535 (1994).

[21] X. Cao and M. Dolg, J. Phys. Chem. A **113**, 12573 (2009).

[22] X. Cao, M. Dolg, and H. Stoll, J. Chem. Phys. **118**, 487 (2003).

[23] T. H. Dunning, J. Chem. Phys. **90**, 1007 (1989).

[24] J. Blaise and J.-F. Wyart, in *International Tables of Selected Constants* (CNRS, Paris, 1992), Vol. 20.

[25] X. Cao and M. Dolg, Mol. Phys. **101**, 961 (2003).